

# CHARACTERIZATION OF PHOTONIC CRYSTAL FIBERS FROM FAR FIELD MEASUREMENTS

Shailendra K. Varshney and R.K.Sinha\*

Dept. of Applied Physics, Delhi College of Engineering  
Faculty of Technology, University of Delhi,  
Bawana Road, Delhi 110 042, India

\*Tele: +91-11-7871015

E-mail: dr\_rk\_sinha@yahoo.com; skvarshney\_10@yahoo.co.uk

## Abstract

We report an online method for characterization of Photonic Crystal Fibers (PCFs) from its far field measurements. PCF is analyzed using effective index method to obtain its far field radiation patterns. It is shown that the normalized frequency ( $V_{\text{eff}}$ ), Core diameter ( $d_{\text{co}}$ ), air hole spacing ( $\Lambda$ ), air hole diameter ( $d$ ) and effective cladding index and hence numerical aperture of PCF can be obtained from its far field measurements.

**Key words:** Photonic Crystal Fiber, Far field, Effective index method

## I. INTRODUCTION

A considerable amount of interest has been generated in Photonic Crystal Fibers [1-3] (PCFs) due to their unusual waveguiding properties like, single mode operation at any wavelength [4], large mode area [5] & manageable dispersion properties [6] etc. Photonic Crystal Fibers are single material optical fibers with a periodic array of air holes running down its length. Such fibers guide light due to a central defect created at a design state. One of the important characteristics of PCFs is single mode operation over an entire range of operating wavelengths, which is, expected to be exploited in various communication and sensing applications in the near future. The other interesting features are control of dispersion in PCFs. As a result, PCF can be designed (i) to exhibit zero dispersion at any wavelength in both Infra-Red & Ultra-Violet regions (ii) provide nearly zero ultraflattened dispersion in the range of 1.3-1.7  $\mu\text{m}$  and (iii) a very high negative dispersion [7-9]. These characteristics of PCF make them useful candidate for Dense Wavelength Division Multiplexed (DWDM) and Dispersion compensation applications. Therefore, with a view of wide applications of PCFs in both existing and futuristic optical fiber networks, an online method for characterization of these fibers is required to be developed. This will help to estimate the design parameters (air hole diameter, air hole spacing, core diameter and  $V_{\text{eff}}$  etc.) of PCF.

The far field radiation pattern of the fundamental mode has been successfully used to characterize single mode step index as well as graded index fibers [10,11]. Further this technique has also been extended in characterization of, step index symmetric slab waveguides [12] & practical integrated optical waveguides [13,14].

Various groups have modeled Photonic Crystal Fibers by different numerical tools [15-20] for determining the waveguiding parameters for lightwave propagation in such fibers. Effective index method is one of them and is used to calculate the effective index (i.e.  $n_{\text{eff}}$ ) of the infinite periodic photonic crystal cladding. The effective normalized frequency (i.e.  $V_{\text{eff}}$ ) of the fiber and dispersion of lightwave signal propagating through PCF has been reported in the literature using effective index approach.

Herein, we describe the development of analytical formulae and a method to characterize PCF from its far field radiation pattern similar to single mode step index fiber using effective index approach.

## II. EFFECTIVE INDEX METHOD

This method is used to determine the cladding mode field by solving the scalar wave equation within a simple cell centered on one of the holes as shown in fig.1 (a). The hexagonal shape of the cell has been approximated by a circular one (as shown in Fig. 1(b)) in order to make a general circular symmetric mode solution.

The solutions in the air hole and silica region is given by

$$\Psi_1 = A I_0(WR) \quad ; R = r/a \quad \text{air hole region; } R > 1$$

$$\Psi_2 = B J_0(RU) + C Y_0(RU) \quad \text{silica region ; } R < 1$$

where 'a' being the radius of the air hole,  $J_0$ ,  $Y_0$  and  $I_0$  are the Bessel functions of first kind, second kind and modified Bessel function of first kind of order zero respectively.

Using boundary condition at the edges, the eigen value equation is obtained as

$$B J_1(u) + C Y_1(u) = 0 \quad (1)$$

where B and C are the constant and is given as

$$B = \frac{A}{J_0(U)} \left[ I_0(W) - \frac{W I_1(W) J_0(U) + U J_1(U) I_0(W)}{U (J_1(U) Y_0(U) - J_0(U) Y_1(U))} \right] \quad (2)$$

and

$$C = \frac{A [W I_1(W) J_0(U) + U J_1(U) I_0(W)]}{U [J_1(U) Y_0(U) - J_0(U) Y_1(U)]} \quad (3)$$

with the parameters U, W and u as follows

$$U = k_0 a \sqrt{n_s^2 - n_{\text{eff}}^2}$$

$$W = k_0 a \sqrt{n_{\text{eff}}^2 - n_a^2}$$

$$u = k_0 b \sqrt{n_s^2 - n_{eff}^2}$$

Here  $n_s$ ,  $n_a$  and  $n_{eff}$  are the refractive indices of pure silica, air and effective index of the cladding respectively.

Therefore, by solving the eigen value equation given by (1), effective index defined by propagation constant of fundamental space filling mode  $\beta_{FSM}$  as  $n_{eff} = \beta_{FSM}/k_0$ , where  $k_0$  is free space propagation constant of light with wavelength  $\lambda_0$ .

The waveguide consists of a core and a cladding region that have refractive indices  $n_{co}$  and  $n_{cl}$  respectively (as shown in Fig1 (b)). The core is pure silica but the refractive index of microstructured cladding region is given by propagation constant of the lowest order mode that propagates in the infinite cladding material.

Now from the knowledge of cladding index ( $n_{cl} = n_{eff}$ ) and known value of core index value ( $n_{co} = 1.45$  i.e.  $n_{silica}$ ), the propagation constant & hence the modal index of guided wave of PCF is obtained similar to step index fiber having core index  $n_{co}$ , core radius,  $\rho$ , and cladding index  $n_{cl} = n_{eff}$ .

## 2.1 PCF as a Step Index Fiber

The fundamental mode solution for the structure as shown in Fig.1 (b) is written as

$$\begin{aligned} \Psi &= AJ_1(UR) & R < 1 \\ &= BK_1(WR) & R > 1 \end{aligned} \quad (4)$$

The constants A and B can be found by applying boundary conditions. Therefore the solution as given by eq.(4) can be rewritten as,

$$\begin{aligned} \Psi &= \frac{1}{J_0(U)} J_1(UR) \\ &= \frac{1}{K_0(W)} K_1(WR) \end{aligned} \quad (5)$$

where  $R = r/\rho$ , and  $\rho \approx 0.64 \Lambda$  [17],  $\Lambda$  is the separation between two air holes called as air hole spacing or pitch

$$U = k_0 \rho (n_s^2 - n_e^2)^{1/2}$$

$$W = k_0 \rho (n_e^2 - n_{cl}^2)^{1/2}$$

### III. FAR-FIELD OF PHOTONIC CRYSTAL FIBER

Since, the mode distribution depends only on radial coordinate ‘r’ of equivalent step index fiber for a given PCF, therefore far field pattern will also be cylindrically symmetric. The modal solution of the wave propagation through PCF is obtained from effective index model as given by the equation (5). These modal fields are used for deriving an expression for far field intensity distribution of lightwave propagating through PCF

The far field amplitude  $u(\theta)$  is given as [21]

$$u = C \int_{-\infty}^{\infty} \int_{-\infty}^{\infty} \Psi(\xi, \eta) e^{ik_0(l\xi + m\eta)} d\xi d\eta \tag{6}$$

where  $l = x/r'$ ,  $m = y/r'$ ,  $l$  &  $m$  are the direction cosines of the observation direction as shown in Fig.2.

Calculating the field distribution along the x axis for which  $m=0$  and  $l=\sin\theta$ , is given as follows:

$$u = C \int_{-\infty}^{\infty} \int_{-\infty}^{\infty} \Psi(\xi, \eta) e^{ik_0 l \xi} d\xi d\eta$$

Substituting,

$$\xi = r \cos \phi ; d\xi = -r \sin \phi d\phi$$

$$\eta = r \sin \phi ; d\eta = r \cos \phi d\phi$$

$$u(\theta) = C \int_{-\infty}^{\infty} \int_{-\infty}^{\infty} r dr \Psi(r) e^{ik_0 r \sin \theta \cos \phi} d\phi \tag{7}$$

Since,

$$J_0(\zeta) = \frac{1}{2\pi} \int_0^{2\pi} e^{i\zeta \cos \phi} d\phi$$

Eq. (4) become,

$$u(\theta) = 2\pi C \int_0^{\infty} r dr \Psi(r) J_0(k_0 r \sin \theta) \tag{8}$$

Eq.8 represents the amplitude of far field pattern at angle  $\theta$ .

Again substituting,  $q = k_0 r \sin \theta = (2\pi/\lambda_0) r \sin \theta$  and  $\alpha=q$   $\rho=k_0 a \sin \theta$ ;  $r = \rho \zeta$  and making use of Eq.2, the far field amplitude is given as

$$u(\theta) = \frac{2\pi C \rho^2}{J_0(U)} \left[ \int_0^1 J_1(U\zeta) J_0(\alpha\zeta) \zeta d\zeta + \frac{J_0(U)}{K_0(W)} \int_1^\infty K_1(W\zeta) J_0(\alpha\zeta) \zeta d\zeta \right] \quad (9)$$

For  $\theta = 0$ , far field amplitude will be,

$$\begin{aligned} u(0) &= \frac{2\pi C \rho^2}{J_0(U)} \left[ \int_0^1 J_1(U\zeta) \zeta d\zeta + \frac{J_0(U)}{K_0(W)} \int_1^\infty K_1(W\zeta) \zeta d\zeta \right] \\ &= \frac{2\pi C \rho^2 U J_1(U)}{U^2 W^2 J_0(U)} V_{eff}^2 \end{aligned} \quad (10)$$

Therefore, normalized far field amplitude  $\tilde{u}(\theta)$  is given by

$$\begin{aligned} \tilde{u}(\theta) &= \frac{u(\theta)}{u(0)} \\ &= \frac{U^2 W^2}{(U^2 - \alpha^2)(W^2 + \alpha^2)} \left[ J_0(\alpha) - \alpha J_1(\alpha) \frac{J_0(U)}{U J_1(U)} \right]; \quad \text{For } U \neq \alpha \\ &= \frac{U^2 W^2}{2V_{eff}^2 U J_1(U)} [J_0^2(U) + J_1^2(U)]; \quad \text{For } U = \alpha \end{aligned}$$

Hence, the normalized far field intensity distribution  $I(\theta)$  will be given by

$$\begin{aligned} I(\theta) &= |\tilde{u}(\theta)|^2 \\ I(\theta) &= \left\{ \frac{U^2 W^2}{(U^2 - \alpha^2)(W^2 + \alpha^2)} \left[ J_0(\alpha) - \alpha J_1(\alpha) \frac{J_0(U)}{U J_1(U)} \right] \right\}^2; \quad \text{For } \alpha \neq U \\ &= \left\{ \frac{U^2 W^2}{2V_{eff}^2 U J_1(U)} [J_0^2(\alpha) + J_1^2(\alpha)] \right\}^2; \quad \text{For } \alpha = U \end{aligned}$$

where  $\alpha = k_0 \rho \sin\theta = (2\pi/\lambda_0) \rho \sin\theta$  and core radius  $\rho = 0.64\Lambda$ , where  $\Lambda$  is the air hole spacings and  $\lambda_0$  is operating wavelength.  $U$  and  $W$  are the fiber parameter for a given value of  $V_{eff}$  for a PCF.

#### IV. CHARACTERIZATION OF PCF

Far field intensity distribution for PCF with normalized radiation angle ( $\alpha$ ) for different values of normalized air hole size ( $d/\Lambda$ ) at a wavelength of 1.55  $\mu\text{m}$  and 1.3  $\mu\text{m}$  are shown in Figures 3 (a) and 3(b) respectively. It is clear from Figures 3(a) and 3(b) that there is shift in the peaks of the first lobe as observed in the far-field radiation patterns. This is because the  $V_{\text{eff}}$  value changes due to change in the wavelength and normalized air hole size ( $d/\Lambda$ ). This indicates that the far field radiation distribution of PCF strongly depends on its relative air hole size.

Universal curve depicting the variation of the ratio of  $\alpha_x/\alpha_h$  ( $= \sin\theta_x/\sin\theta_h$ ) and normalized half intensity angle  $\alpha_h$  ( $= k_0 \rho \sin\theta_h$ ) with  $V_{\text{eff}}$  for different structures of equivalent step index fibers for given PCFs are shown in Figure 4.

$\theta_x$  is the angle corresponding to first minima of the far field pattern and  $\theta_h$  represents the angle where the far field intensity drops to half of its maximum.

It is here emphasized that the far field intensity distribution of PCF is similar to that of the single mode step index fiber. However, the difference lies to the fact that in case of PCF the far field intensity distribution is observed with effective  $V_{\text{eff}}$  value and not with the absolute  $V$  value. Thus, on measuring the angles  $\theta_x$  and  $\theta_h$  the ratio of  $\sin\theta_x/\sin\theta_h$  is obtained, from where  $V_{\text{eff}}$  of PCF can be obtained from Fig.4.

Further with the knowledge of  $V_{\text{eff}}$  of PCF the normalized half intensity angle  $\alpha_h$  can be determined and hence the core radius ' $\rho$ ' can be determined. Since,  $\rho=0.64\Lambda$ , therefore, air hole spacings  $\Lambda$  of a given PCF can be obtained. Now, with the knowledge of  $V_{\text{eff}}$ , core radius and operating wavelength ( $\lambda$ ), the effective cladding index of PCF can be known by knowing the refractive index of core. In case of PCF, the core is pure silica and its refractive index is known at any wavelength. Hence, the effective cladding index of PCF can be estimated. Again by knowing the core index and effective cladding index, numerical aperture (i.e.  $(n_s^2 - n_{cl}^2)^{1/2}$ ) of PCF can be obtained.

From Figure 5, the normalized air hole size can be estimated by knowing the effective normalized frequency of PCF from Fig. 4. Since, air hole spacing is already estimated, hence, air hole diameter can be determined. Thus, with the help of figures 3,4 and 5, all the essential design parameters of PCF can be obtained.

#### V. CONCLUSION

An effective index method has been applied to characterize Photonic Crystal Fibers from its far field radiation patterns similar to the conventional step index fiber. In this method, a PCF is approximated to step index fiber. The universal curves are obtained for different designs of PCFs, which is used to determine the additional parameters (air hole size, effective cladding index and air hole spacings) of PCF.

#### Acknowledgements

The authors gratefully acknowledge the financial support provided by All India Council for Technical education (A.I.C.T.E), Govt. of India for the work under R&D project "Characterization of Photonic Crystal Fibers and waveguide for Telecom & Sensing Applications"

One of the authors (Shailendra Kumar Varshney) also acknowledges the financial support provided by University Grants Commission (UGC), Govt. of India.

## REFERENCES

- [1] J. C. Knight, T. A. Birks, R. F. Cregan and P. St. J. Russell, "Photonic crystals as optical fibers-Physics and applications," *Opt. Mater.* Vol.11, (1998), pp. 143-151
- [2] J. Broeng, D. Mogilevstev, S. E. Barkou and A. Bjarklev, "Photonic Crystal Fibers: A new class of optical waveguide," *Opt. Fiber Technol.*, Vol. 5, (1999), pp. 305-330
- [3] R. Ghosh, A. Kumar, J. P.Meunier and E. Marin, "Modal characteristics of few-mode silica-based photonic crystal fibers," *J. Opt. & Quantum Electron.* Vol. 32, (2000), pp. 963-970
- [4] T.A.Birks, J.C.Knight and P.St.J.Russell, "Endlessly single mode Photonic crystal fiber" *Opt.Lett.*22 (1997) 961-963
- [5] J. C. Knight, T. A. Birks, R. F. Cregan, P. St. J. Russell and J. P. de Sandro, "Large mode area photonic crystal fiber," *Elect. Lett.* Vol. 34, (1998), pp. 1347-1348
- [6] Tanya M. Monro, D.J.Richardson, N.G.R.Broderick and P.J.Bennett, "Holey Optical Fibers: An Efficient Modal Model", *J. Lightwave Technol.*, 17(1999) 1093-1101
- [7] A. Ferrando, E. Silvestre, J.J.Miret and P. Andres, "Nearly zero ultraflattened dispersion in photonic crystal fibers," *Opt. Lett.* Vol. 25, (2000), pp. 790-792
- [8] T. A. Birks, D. Mogilevstev, J. C. Knight and P. St. J. Russell, "Dispersion compression using single material fibers," *Photon. Technol. Lett.* Vol. 11, (1999), pp. 674-676
- [9] R. K. Sinha and Shailendra K Varshney, "Dispersion properties of Photonic crystal fibers," submitted for publication in *Microwave & Optical Technology Letters*
- [10] W.A. Gambling, D.N. Payne, H. Matsumura and R.B. Dyott, *IEE J Microwave Opt. and Acoust.*,1(1976) 13.
- [11] A.K.Ghatak, R. Srivastava, I.F. Faria, K.Thyagarajan and R. Tewari, *Electronics Letters*, Vol.19(1983) pp. 97-98.
- [12] A.C. Boucouvalas, *Electronics Letters*, Vol. 19(1983) 120-121
- [13] A. Kumar and R.K. Sinha, "Characterization of single mode channel waveguides from far field measurements", *Optics Communications*, Vol. 36 (1987) pp. 89-93
- [14] R.K.Sinha and S.I.Hosain, "Characterization of single mode asymmetric slab waveguide from far field intensity pattern", *J. Opt. Commun.* Vol. 10, (1989) pp. 105-107
- [15] A. Ferrando, E. Silvestre, J.J. Miret, P.Andres and M. V. Andres, "Full-vector analysis of a realistic Photonic crystal fiber" *Opt. Lett.* Vol. 24 (1999) pp. 276-278.
- [16] E. Silvestre, J.J. Miret, P.Andres and M. V. Andres, "Biothonormal-basis method for the description of optical fiber modes" *J. Lightwave Technol.* Vol. 16(1998) pp. 923-928
- [17] F. Brechet, J. Marcou, D. Pagnoux and P. Roy, " Complete analysis of the propagation characteristics into Photonic Crystal Fibers by the Finite Element Method", *J. Opt. Fiber Technology*, Vol. 6(2000) pp. 181-191
- [18] M. Qiu, "Analysis of guided modes in photonic crystal fibers using the finite difference time domain method," *Microwave Opt. Technol. Lett.* Vol. 30, (2001) pp. 327-330
- [19] Z. Zhu and T. G. Brown, "Full-vectorial finite-difference analysis of microstructured optical fibers," *Opt. Express*, Vol. 10, (2002) pp. 853-864
- [20] A. Ghatak, K. Thyagarajan, *Introduction to Fiber Optics*, Cambridge University Press, UK, 1999.

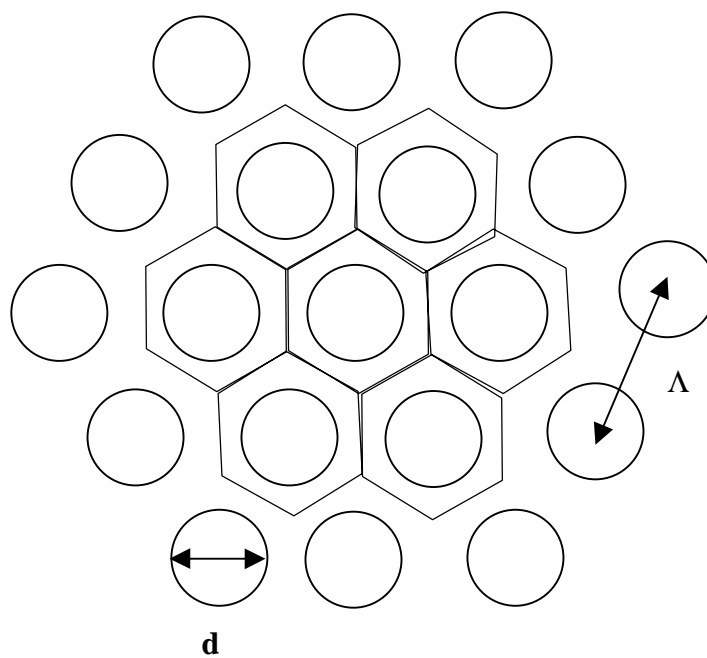


Fig. 1(a) Cross-section of triangular photonic crystal with air hole diameter 'd' and spacing between two air holes as 'Λ' composed of hexagonal unit cell

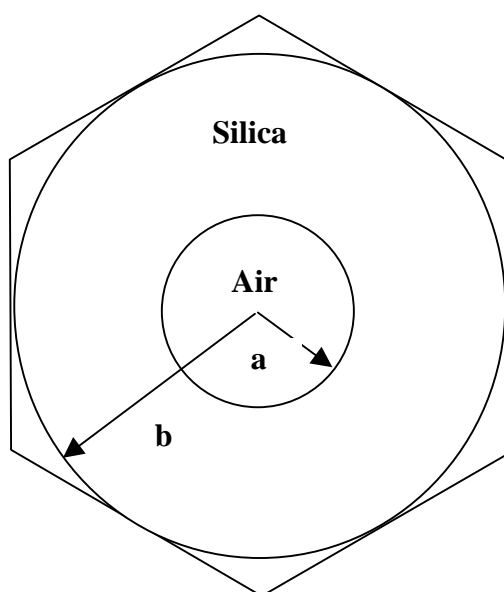


Fig. 1(b) Circular approximation of hexagonal unit cell (air in silica structure)



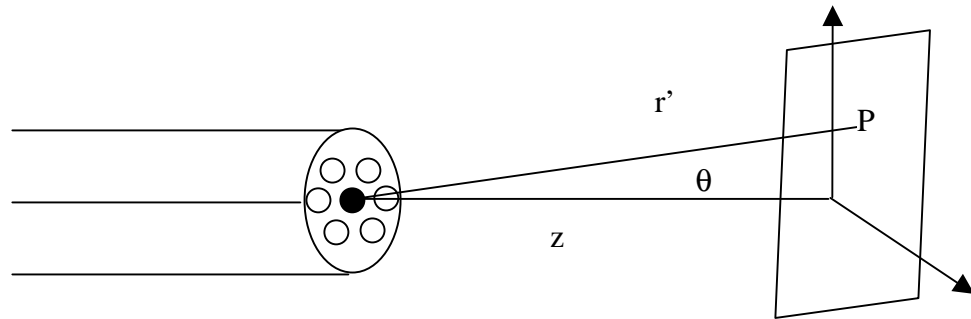


Fig 2 Far-field radiation pattern with observation point P and angle  $\theta$ .

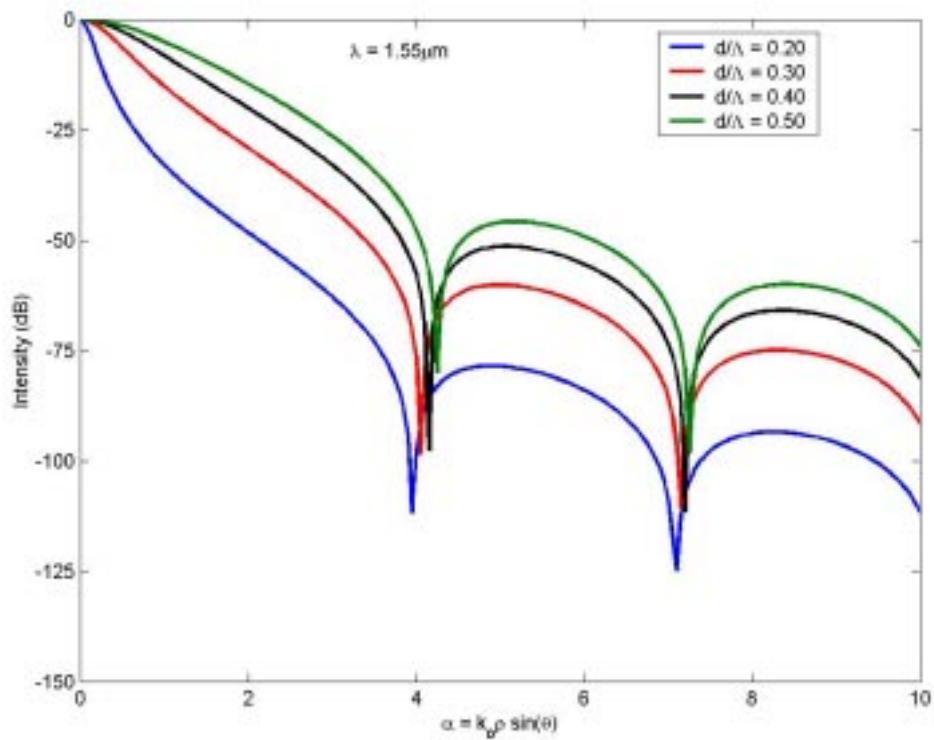


Fig. 3(a) Far-field intensity pattern of Photonic Crystal Fibers having  $d/\Lambda = 0.20, 0.30, 0.40$  having core radius  $0.64\Lambda$  at a wavelength of  $1.55\mu\text{m}$

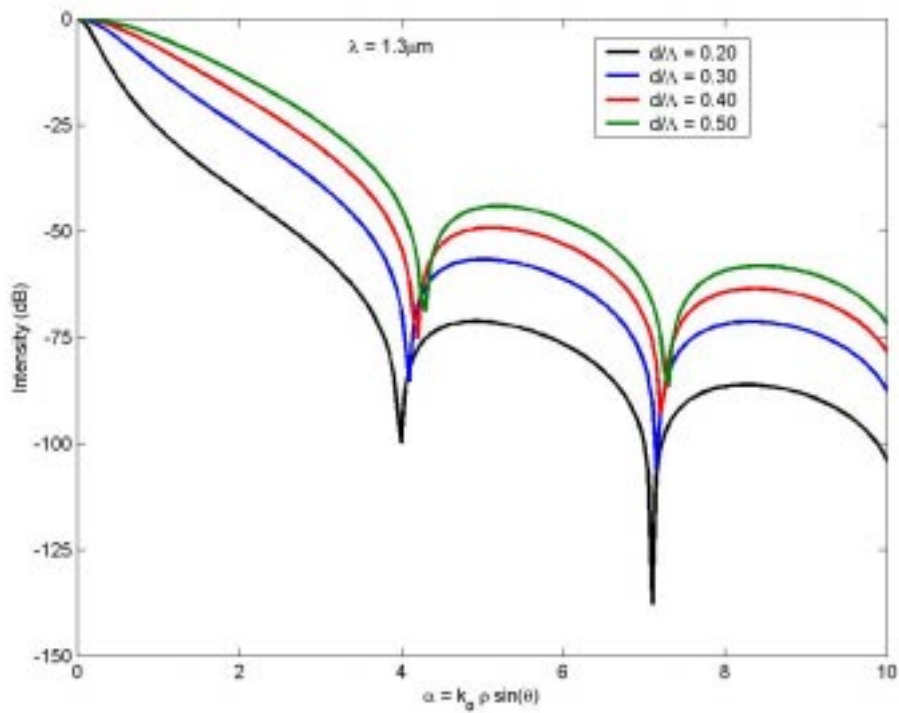


Fig 3(b) Far-field intensity pattern of Photonic Crystal Fibers having  $d/\Lambda = 0.20, 0.30, 0.40$  having core radius  $0.64\Lambda$  at a wavelength of  $1.3\mu\text{m}$

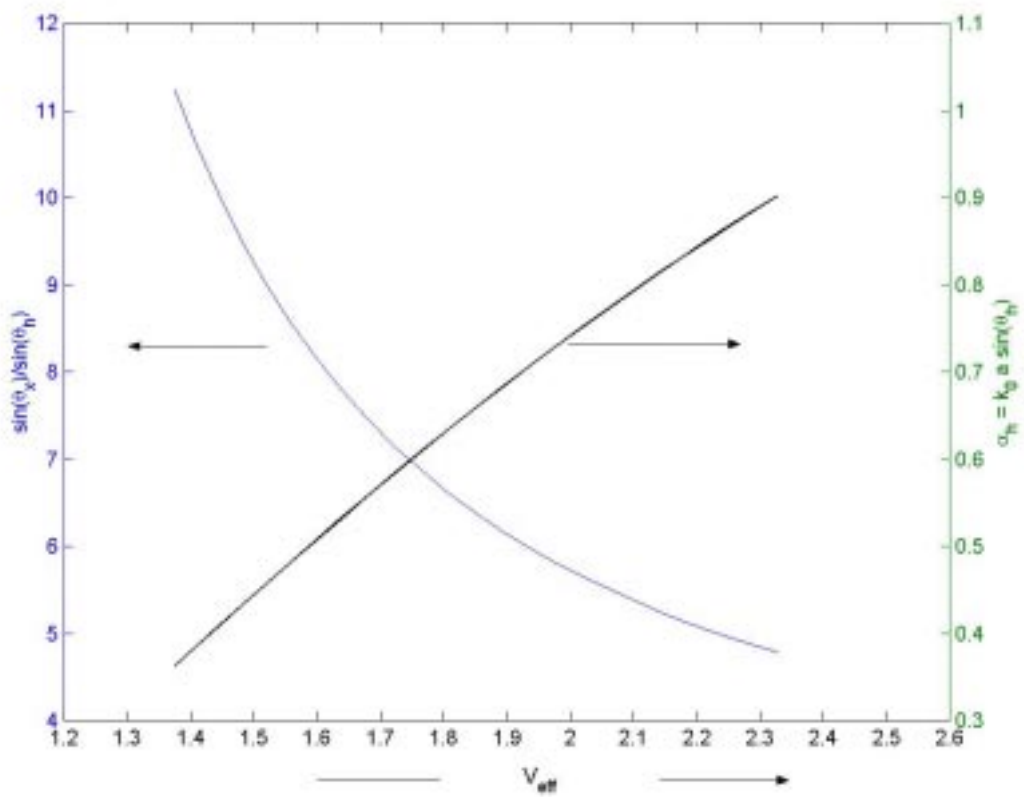


Fig. 4 Universal curves depicting the variation of  $\sin\theta_x/\sin\theta_h$  and  $k_0\rho \sin\theta_h$  with  $V_{\text{eff}}$  for equivalent step index fiber for given PCF

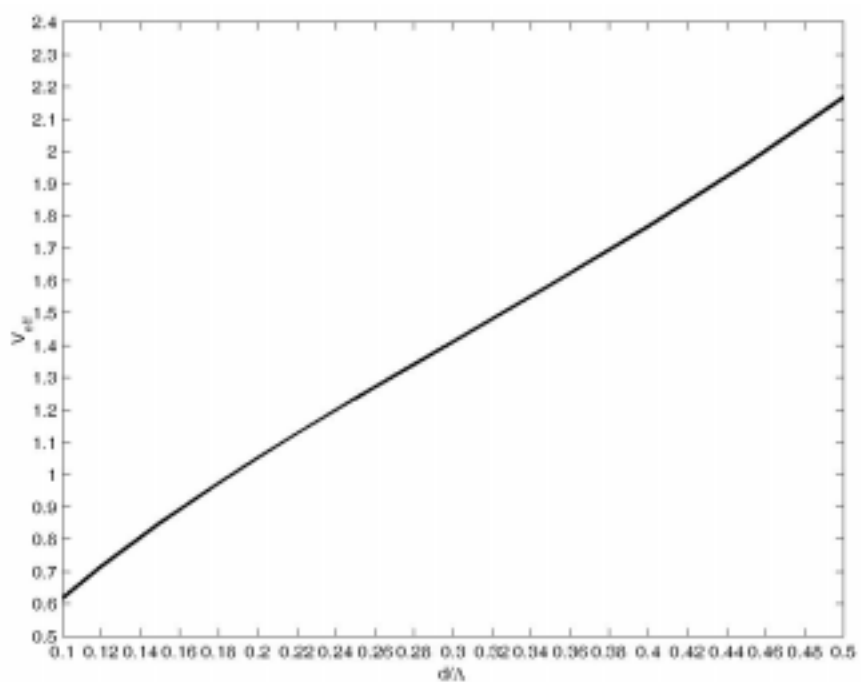


Fig. 5: Variation of effective normalized frequency ( $V_{eff}$ ) as a function of normalized air hole size ( $d/\Lambda$ )